

# AFM study of austeno-ferritic stainless steel microstructure after cathodic hydrogen charging

A. Głowacka\*, M.J. Woźniak, W.A. Świątnicki

*Warsaw University of Technology, Department of Materials Science & Engineering,  
Woloska 141, 02-507 Warsaw, Poland*

Received 1 June 2004; received in revised form 7 February 2005; accepted 9 February 2005  
Available online 14 July 2005

## Abstract

Microstructural changes occurring in austenitic–ferritic stainless steel after two variants of thermo-mechanical treatment and subjected to cathodic hydrogen charging were studied using atomic force microscopy operated in the magnetic force imaging mode. Hydrogen-induced phase transformations were observed to occur in both steel variants. In austenite, they were manifested by the formation of  $\alpha'$  martensite magnetic laths. In ferrite, the microstructural changes resulted in a pronounced surface relief being formed.

© 2005 Elsevier B.V. All rights reserved.

*Keywords:* Metals; Magnetic measurements; Atomic force microscope

## 1. Introduction

Hydrogen-induced microstructural changes, and as a consequence, changes of mechanical properties, can be very important in the exploitation of materials. Although, so far, many observations have been made, there are still many doubts concerning the sequence of the microstructural transformations, the formation of new phases and their genesis. In our work, we focused on the austeno-ferritic stainless steels, which have an improved resistance to corrosion cracking compared with that of austenitic stainless steels, but they suffer from hydrogen embrittlement (HE) in aqueous solutions. Our earlier studies allowed us to distinguish various microstructural [1,2] and phase [3] transformations generated in the  $\gamma$  and  $\alpha$  phases. Now, our concern is focused on the influence of the initial microstructure on the steel behaviour under cathodic hydrogen charging, using an atomic force microscope (AFM).

## 2. Experimental

The material used in this study was Cr23–Ni5–Mo3 austeno-ferritic stainless steel (chemical composition in wt.%: 0.026 C, 0.35 Si, 1.57 Mn, 5.43 Ni, 22.94 Cr, 2.75 Mo, 0.164 N, 0.001 S, 0.021 P, 0.012 Al).

The material was subjected to a thermo-mechanical treatment applied in two variants A and B (see Table 1) in order to produce two series of specimens (A and B), containing the same volume fractions of austenite and ferrite of about 50% but with different types of orientation relationships (ORs) between the  $\alpha$  and  $\gamma$  phases.

Generally, the A treatment led to the precipitation of the  $\gamma$  phase in the form of elongated grains embedded in the ferritic matrix. In this case, the grain size of the ferritic phase is basically bigger (up to 100  $\mu\text{m}$ ). With the B treatment, a fully recrystallized, duplex microstructure with equiaxed  $\alpha$  and  $\gamma$  grains of approximately, 3–5  $\mu\text{m}$  in diameter was obtained.

An EBSD analysis of the interphase boundaries (IBs) structure revealed that, in state A, most of the  $\gamma$  grains have orientations close to the Kurdjumov–Sachs (K–S), Nishiyama–Wassermann (N–W) or to the Greninger–Trojano (G–T) ORs with respect to the ferritic matrix [4]. It should

\* Corresponding author. Tel.: +48 22 660 83 79; fax: +48 22 660 87 05.  
E-mail address: annabur@inmat.pw.edu.pl (A. Głowacka).

Table 1  
Schematic description of the thermo-mechanical treatments

Treatment	A	B
Step 1	bar drawing	bar drawing
Step 2	annealing 1260 °C–30 mn in argon atmosphere, water quenching	
Step 3	annealing 1000 °C–2 h in argon atmosphere, water quenching	

be emphasized that the difference between the K–S or N–W and G–T ORs is very small ( $2.5^\circ$ ), which make them hard to distinguish [5]. In state B, the recrystallisation that occurs during  $\gamma$  growth destroys the habitual N–W and K–S orientation relationships between the  $\gamma$  and  $\alpha$  phases and leads to a more random misorientation between these phases. This means that the main difference between the two states results in special IBs structure that is characterized by low energy in state A (where the IBs fulfill special ORs) and is random in state B (for which the IBs deviate from special ORs) [6].

Samples in the form of bars (8 mm in diameter) were machined to reduce their diameter to 3 mm and next sliced to 0.2 mm thick discs using a wire saw. Finally, they were polished to thin foils by two-sided electrolytic thinning.

Hydrogen charging of the thin foils was carried out electrolytically at room temperature in a 0.1 M  $\text{H}_2\text{SO}_4$  aqueous solution with an addition of 10 mg/l of a hydrogen entry promoter ( $\text{As}_2\text{O}_3$ ). A current density of 20 mA/cm<sup>2</sup> was applied between the specimen and a platinum anode.

The topographic and magnetic features of the DSS samples before and after hydrogen charging were examined with a Multi Mode AFM NanoScope IIIa Digital Instruments.

The AFM was operated in the magnetic force imaging mode (MFM). During the MFM measurement the microscope collected simultaneously the topographic image (in tapping mode) and the image of the magnetic interaction between the microscope tip and the sample surface (in lift mode). The magnetic image was collected in the Phase Detec-

tion and Frequency Modulation Modes. The MESP-HM tips (for high moment materials), coated with a cobalt alloy, were used. More details of the AFM experimental technique can be found in reference [7].

### 3. Results

The AFM observations allowed us to investigate the microstructure of both types of steel at three stages: (1) before the cathodic hydrogen charging, (2) just after the charging, and (3) after hydrogen desorption. The initial microstructure of the A and B steel states, shown in Figs. 1 and 2, was taken using the topography and magnetic modes. In each case, the ferrite and austenite phases were clearly visible. With the topography mode, it was the  $\gamma$  phase, which was etched out during the sample preparation, and was thus concave. In the magnetic mode, the ferromagnetic  $\alpha$  phase appeared dark and the paramagnetic  $\gamma$  phase-bright.

The hydrogen charging induced great changes in the microstructure of the steel. The investigations performed just after the hydrogen charging revealed some changes in the  $\alpha$  phase. Generally, a pronounced needle-shaped relief was observed. The changes in  $\gamma$  phase appeared in the form of magnetic laths after hydrogen desorption (Figs. 3 and 4). The main difference between the A and B states of the steel consisted in the time necessary for this magnetic transformation occurrence. In the case of A state, magnetic laths in the austenite appeared 3–4 h after the end of the hydrogen charging, while in the B state they formed not earlier than 72 h after hydrogenation process. It also seemed that in case of B state, the size of the needle-shaped structures in the ferrite was strictly connected with the grain diameter and gained about 4–5  $\mu\text{m}$ . This effect was not observed in the A state, where needles were much smaller than the grain diameter but also their sizes varied from 1  $\mu\text{m}$  and even 20  $\mu\text{m}$ .

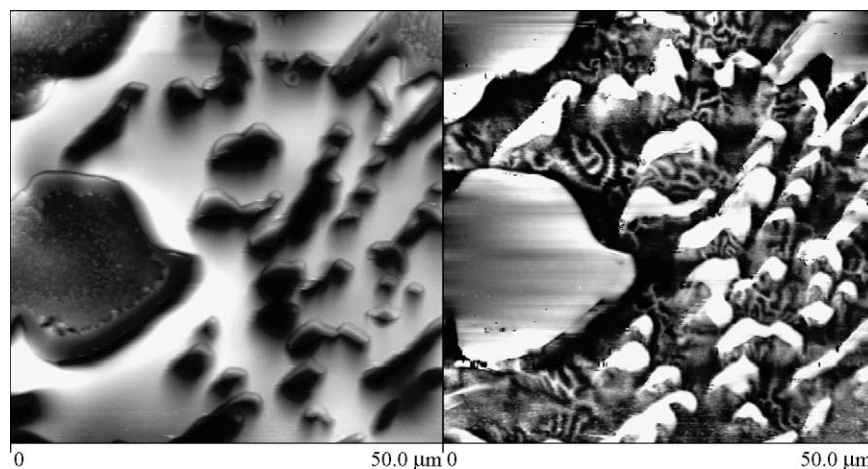


Fig. 1. Initial microstructure of state A before hydrogen charging: (a) in topography and (b) magnetic modes. In topography mode, the ferrite phase  $\alpha$  appeared bright and the austenite  $\gamma$  appeared dark. In the magnetic mode the contrast of the phases was inverted:  $\alpha$  was dark and  $\gamma$  was bright.

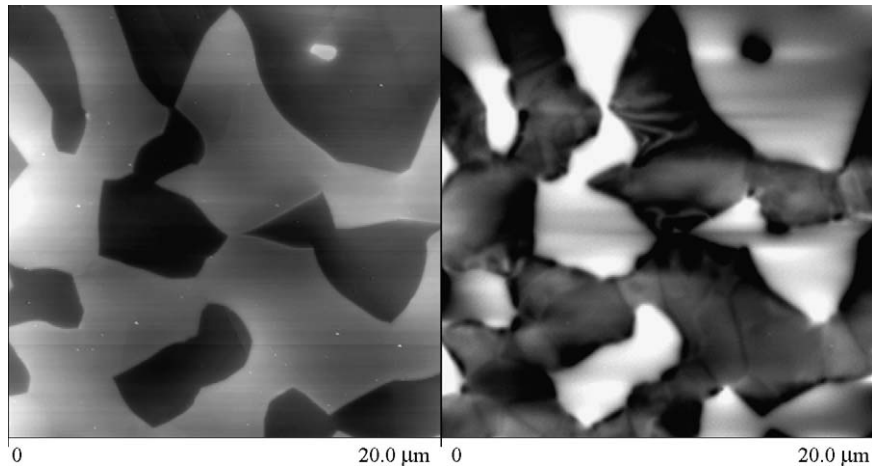


Fig. 2. Initial microstructure of state B before hydrogen charging in (a) topography and (b) magnetic modes. In topography mode, the  $\alpha$  phase appeared bright, the  $\gamma$  appeared dark. In the magnetic mode the contrast of the phases was inverted:  $\alpha$  was dark and  $\gamma$  was bright.

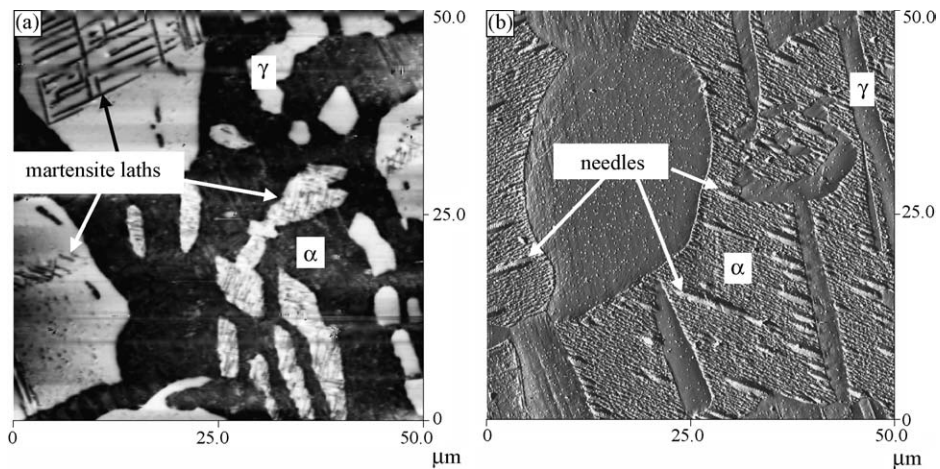


Fig. 3. Microstructure of state A after hydrogen desorption: (a) magnetic mode—dark, magnetic laths of martensite  $\alpha'$  in a paramagnetic austenite grains; (b) topography mode — needle-shaped features in ferrite grains.

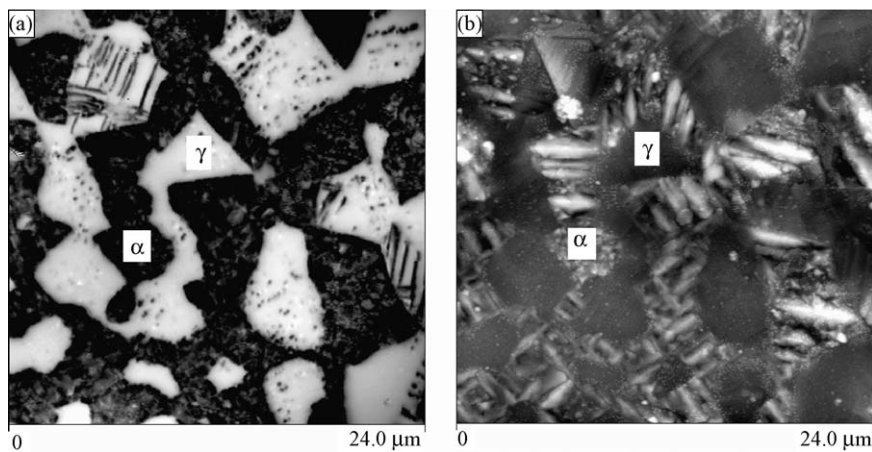


Fig. 4. Microstructure of state B after hydrogen desorption. (a) magnetic mode - dark, magnetic martensitic laths in paramagnetic austenite grains; (b) topography mode – needle-shaped features in ferrite grains.

The influence of the ORs between the two phases on the hydrogen embrittlement resistance of the steel was not observed. The expected generation of microcracks on the IBs in state B was not confirmed.

#### 4. Discussion

As stated in our earlier paper [3], the laths observed in the  $\gamma$  phase were caused by the occurrence of the isothermal martensitic transformation. In austenitic steels, two different martensitic transformations:  $\gamma \rightarrow \alpha'$  and  $\gamma \rightarrow \varepsilon$  were observed. The martensite  $\alpha'$  is the body centred cubic (bcc), ferromagnetic phase, while  $\varepsilon$  is the hexagonal close packed (hcp), paramagnetic phase. Our AFM observations confirms the formation of  $\alpha'$  martensite in Cr23–Ni5–Mo3 steel after cathodic hydrogen charging and hydrogen desorption. However, the time necessary for the appearance of the martensitic laths suggests that the whole process is more complex. Detailed investigations performed by Szummer [8] seem to confirm this hypothesis. He claimed the formation of a short-living hydride phase prior to the martensitic transformation. Moreover, Lublinska and Szummer [9] reported the occurrence of a short-living hydride phases in austenite of duplex stainless steel (Cr17–Ni5–Mo3–Si2), but followed by the formation of a stable  $\varepsilon$  martensite during hydrogen desorption. They did not find the  $\alpha'$  martensite. Yang et al. [10] who examined 304 stainless steel suggested that martensite  $\varepsilon$  formed during hydrogen charging, and the  $\alpha'$  phase appeared during aging, by a  $\varepsilon \rightarrow \alpha'$  transformation. It is well known that the stacking faults in the  $\gamma$  phase have been recognized as the nucleation sites for martensitic transformation. Therefore, we can suppose that a similar transformation also takes place in the Cr23–Ni5–Mo3 steel, but the paramagnetic  $\varepsilon$  phase cannot be revealed in the magnetic mode. Our earlier transmission electron microscope studies [1,2] also seemed to confirm this mechanism taking into account an observed increase of stacking faults density in the austenite after the first minutes of hydrogen charging.

However, the faster formation of the  $\alpha'$  martensite in state A needs some more explanation. Because the IBs formed in special ORs are semi-coherent, they introduce stresses, which may additionally favour the martensitic transformation. It is also possible that the  $\alpha$  grains may act as the nuclei of the  $\alpha'$  martensite, oriented in K–S or N–W ORs with respect to austenite, similarly as the  $\alpha$  and the  $\gamma$  grains in this state. Assuming, that the nucleation process takes place on the IBs, the  $\alpha'$  phase can take advantage of favorably oriented  $\alpha$  phase and grow more quickly. This effect is not possible in state B with the random ORs. If the interfacial stresses are absent and favorably oriented  $\alpha$  grains, which may act as the nuclei, do

not exist, then the transformation to  $\alpha'$  martensite is harder to occur.

#### 5. Conclusions

The occurrence of a martensitic transformation in the austenite phase of two states of Cr23Ni5Mo3 austeno-ferritic stainless steel was revealed. A difference between the A and B states existed in the time necessary for the occurrence of the martensitic transformation. It was also shown that, in the ferrite grains of both states, the formation of surface relief took place.

Atomic Force Microscope working in topography and magnetic modes proved to be an effective tool in the investigation of hydrogen induced microstructural changes.

The influence of the ORs between two phases on the hydrogen embrittlement resistance of the steel was not confirmed.

#### Acknowledgement

This work was supported by Warsaw University of Technology. Authors also wish to thank Polish Committee of Scientific Researches (KBN) for supporting this work.

#### References

- [1] A. Głowacka, W.A. Świątnicki, Mater. Chem. Phys. 81 (2003) 496–499.
- [2] A. Głowacka, W.A. Świątnicki, J. Alloys Compd. 356–357 (2003) 701–704.
- [3] A. Głowacka, W.A. Świątnicki, E. Jezierska, in: Proceedings of the XII International Conference EMS'2005, Kazimierz, Poland, 2005.
- [4] G. Nolze, A. Głowacka, W. Świątnicki, in the report on the Polish Committee of Scientific Researches (KBN) project no 7 T08A 003 20, "The influence of hydrogen on the structure of  $\alpha / \gamma$  interphase boundaries and on the mechanical properties of austenitic-ferritic steel", Warsaw, 2004.
- [5] U. Dahmen, Acta Metall. 30 (1982) 63–73.
- [6] W.A. Świątnicki, Structural Foundations of Interface Engineering (in polish), Oficyna Wydawnicza Politechniki Warszawskiej, Warsaw, 2003.
- [7] M.J. Woźniak, A. Głowacka, J.A. Kozubowski, J. Alloys Compd., in press.
- [8] A. Szummer, Hydrogen Degradation of Ferrous Alloys, Noyes Publications, Park Ridge NJ, USA, 1985, pp. 512–534.
- [9] K. Lublinska, A. Szummer, in: Proceedings of the II Conference Korozja '90, Wrocław, 1990, pp. 107–111.
- [10] Q. Yang, L.J. Qiao, S. Chiovelli, J.L. Luo, Scripta Mater. 40 (1999) 1209–1214.